Journal of Physics: Conference Series

PAPER • OPEN ACCESS

Coupled modeling of wake steering and platform offsets for floating wind arrays

To cite this article: Ericka Lozon *et al* 2024 *J. Phys.: Conf. Ser.* **2767** 062035

View the article online for updates and enhancements.

You may also like

- Predicting the benefit of wake steering on the annual energy production of a wind farm using large eddy simulations and Gaussian process regression
Daan van der Hoek, Bart Doekemeijer, Leif Erik Andersson et al.
- Field Validation of Wake Steering Control with Wind Direction Variability
Eric Simley, Paul Fleming and Jennifer King
- The potential role of airborne and floating wind in the North Sea region
Hidde Vos, Francesco Lombardi, Rishikesh Joshi et al.

This content was downloaded from IP address 192.174.37.51 on 02/07/2024 at 03:06

Journal of Physics: Conference Series **2767** (2024) 062035 doi:10.1088/1742-6596/2767/6/062035

Coupled modeling of wake steering and platform offsets for floating wind arrays

Ericka Lozon[1], **Matthew Hall**[1], **Mohammad Youssef Mahfouz**[2]

[1] National Renewable Energy Laboratory (NREL), 15013 Denver W Pkwy, Golden, CO 80401, United States
[2] Stuttgart Wind Energy at University of Stuttgart, Allmandring 5B, 70569 Stuttgart, Germany

E-mail: ericka.lozon@nrel.gov

Abstract. Wake effects are a key challenge in the design and analysis of wind farms. For floating wind farms, the platforms offset under the aerodynamic loading of the turbine and are constrained by mooring systems that can vary significantly in allowable offsets. When considering wake steering, the crosswind offset of the turbine can counteract the lateral deflection of the wake. This work presents a tool to efficiently model the coupled impacts of wake steering and platform offsets for floating wind farms. The tool relies on the frequency-domain wind farm model RAFT and the steady-state wake model FLORIS. A verification with FAST.Farm is presented, then the tool is applied to a simple two-turbine case study. A range of mooring systems with increasing platform offsets and varied yaw misalignment angles are considered while comparing the impact on turbine power. Additional sensitivities to turbine spacing and mooring system orientation are explored. The results show that there is a least-optimal watch circle width for downwind turbine power production that varies with yaw misalignment angle and turbine spacing. Additionally, the turbine offsets under yaw-misaligned conditions vary significantly depending on mooring system orientation relative to the rotor plane, which in turn impacts the optimal misalignment angle. These results highlight the importance of including floating platform offsets and mooring systems in the evaluation of wake steering strategies for floating wind arrays.

1 Introduction

Wake effects are an important consideration when modeling floating wind arrays. Downwind turbines experience lower wind speeds, which reduces the mean aerodynamic load. The change in turbine loading consequently impacts both the floating platform offset, relative to the platform's undisplaced position, and mooring line loads. Accurately modeling wake losses is especially important when considering wake steering. Wake steering is a method to mitigate wake losses in certain wind directions by operating turbines in a misaligned state to direct the wakes laterally so that they avoid downwind turbines. For fixed-bottom turbines, wake steering has been shown to enable overall energy yield increases typically in the range of 3–5% [1] [2].

Previous studies have evaluated wake effects in floating arrays, considering the coupled nature of rotor aerodynamics and platform motions. Wise and Bachynski [3] looked at the effects of wake meandering on the motions and loads of a pair of floating wind turbines using FAST.Farm. They consider three support structure types and focus especially on response dynamics. They found that lateral wake meandering was not specific to the platform, but vertical meandering increased with larger mean

Content from this work may be used under the terms of the Creative Commons Attribution 4.0 licence. Any further distribution of this work must maintain attribution to the author(s) and the title of the work, journal citation and DOI.
Published under licence by IOP Publishing Ltd

platform pitch angles. Van Binsbergen et al. [4] took a similar approach by simulating two aligned turbines in FAST.Farm to investigate power production and especially drivetrain loads. They considered yaw misalignment angles ranging from 5° to 10° and found that the maximum power increase occurs for a yaw angle of 7° in the upwind turbine. Johlas et al. conducted large eddy simulations of floating wind turbines with an actuator line model coupled to OpenFAST [5]. They compared the wake characteristics between a fixed turbine and floating wind turbines with two substructure types: spar and semisubmersible. The results showed that floating turbine wakes are deflected upward due to the mean platform pitch, but the wake characteristics are otherwise similar between fixed and floating wind turbines.

For floating wind turbines, the benefits of wake steering need to be reevaluated because the yaw misalignment of a turbine increases the crosswind component of its aerodynamic forces, causing the turbine to drift laterally in the direction opposite to the wake steering. This phenomenon potentially reduces the wake steering effectiveness. This effect is included in some existing studies, such as Kheirabadi and Nagamune [6], where they induced desired turbine repositioning using nacelle yaw misalignment and axial induction. They developed a model that combines FLORIS (a steady-state wind farm wake model) with a newly derived two-dimensional wind turbine model, then conducted an optimization process to determine axial induction factors and nacelle yaw angles that maximize farm power. Their results show that the wind farm efficiency gain is increased as the mooring line lengths and resulting platform offsets are increased. More recently, Kheirabadi and Nagamune extended this work, concluding that increasing anchoring radius is necessary for achieving compliant mooring systems and adequate wake offsetting [7]. Additionally, they found that for a three-line uniformly spaced mooring system, a directly upwind line is ideal for wind farm efficiency gains, and the method is only effective for orientations ±20° from this optimum. These previous studies focused mostly on highly compliant mooring systems where the primary goal is lateral repositioning rather than wake steering. The relationship between floating platform offsets and wake steering remains a topic in need of exploration. To address this challenge, we develop and apply a new computationally efficient modeling capability that makes it easier to study the combined effects of wakes and floating turbine offsets. The modeling capability is first verified with a FAST.Farm simulation to confirm accurate platform offsets and turbine power in yaw-misaligned scenarios. Then, we apply the tool to evaluate the effect of the lateral offsets of floating wind turbines on wake steering benefits through a two-turbine case study. We consider a range of mooring systems with varied stiffness and resultant platform offsets, as well as varied yaw misalignment angles. Further, the sensitivities to turbine spacing and mooring system orientation relative to wind direction are evaluated.

2 Methodology

To develop this modeling capability, we rely on the frequency-domain floating wind turbine simulation tool RAFT [8]. To incorporate wake effects in the RAFT array model, we couple RAFT with FLORIS, a steady-state wake modeling tool [9]. The coupling is set up so that RAFT supplies FLORIS with array layout information and key turbine parameters, including power and thrust coefficient curves that account for the pitch of the floating platform. The coupling also supplies FLORIS with a lookup table of wind speed and pitch angle, which RAFT calculates for the wind turbine model. This allows for the modeling of vertical wake deflection, if an appropriate FLORIS wake model is chosen.

To solve for the floating wind turbine positions and wake losses, we set up an iterative process. First, RAFT computes the initial turbine positions at the upstream wind speed. The floating offset positions are passed to FLORIS, where the wake losses and downstream wind speeds are calculated. The updated wind speeds are then passed back to RAFT, where the final turbine positions account for both wake losses and the floating offsets. A flowchart of this iterative process is shown in Figure 1.

As part of this work, we expanded RAFT's capabilities to include support for yaw misalignment. RAFT obtains the wind turbine aerodynamic loads using CCBlade, a steady-state solver using blade element momentum theory that accounts for turbine pitch and yaw misalignment [10]. Accordingly, the mean turbine pitch angle and the yaw misalignment (based on the wind direction and a user-specified turbine yaw angle) are both passed to CCBlade, such that both angles are accounted for when computing the overall turbine aerodynamic forces and moments, as well as the derivatives that RAFT uses when computing the dynamic response. All six degrees of freedom of the aerodynamic forces are included when computing the equilibrium position in RAFT. We created a similar expansion in the coupling to FLORIS, such that the same nacelle yaw angles used by RAFT for CCBlade are also passed to FLORIS. FLORIS internally handles the impact of the yaw misalignment angle on the power generation and wake field. Using the above handling of yaw misalignment for both CCBlade and FLORIS, we can then use RAFT to calculate crosswind offsets for cases with wake steering, allowing a

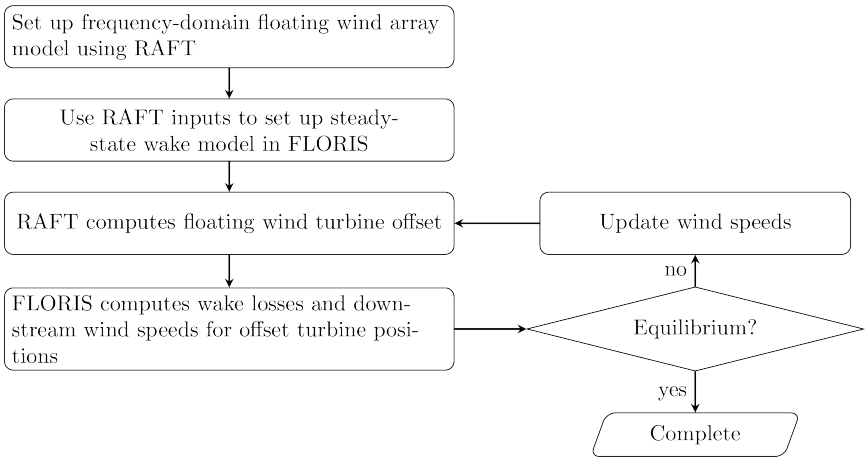

Figure 1: Flowchart showing RAFT and FLORIS coupling

rapid assessment of the wake effects on downstream turbines in floating scenarios. In this work, we assumed that the controller would internally account for the platform yaw, so the yaw misalignment angles in this paper are inclusive of platform yaw.

3 Verification

The coupled modeling capability is verified using FAST.Farm [11], the National Renewable Energy Laboratory's time-domain wind farm simulation tool, to ensure accuracy in the resulting platform offsets and wake losses. To verify, we set up an array of four wind turbines with uniform 1800 m spacing. The IEA 15 MW wind turbine [12] and the VolturnUS-S semisubmersible [13] are used. The mooring system is a generic, semi-taut mooring system designed for an 800 m water depth. The array is shown in Figure 2 with turbine labels.

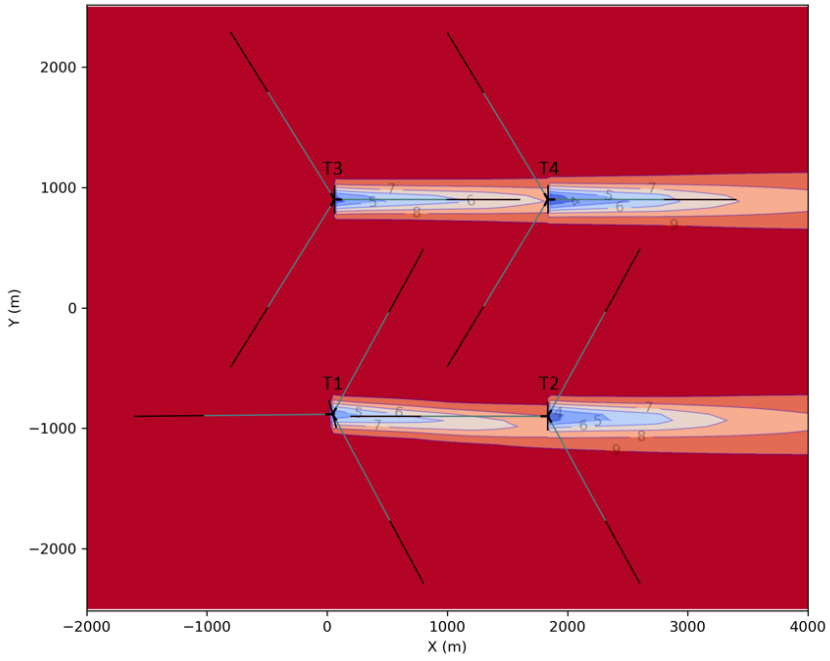

Figure 2: Floating array layout for verification with FAST.Farm

The array is modeled with a 10 m/s wind speed with a turbulence intensity of 0.06, applied so that the wind heading is toward the positive x-axis (X). Turbines 1 and 2 have a mooring line directly upwind, and turbines 3 and 4 have a line directly downwind. Turbine 1 has 15° of yaw misalignment, which is a counter clockwise rotation of the nacelle relative to the wind direction, while the rest of the turbines have zero yaw misalignment. In FLORIS, the Gaussian Curl Hybrid (GCH) model is used, which does not include vertical wake deflection [14]. In FAST.Farm, the curled wake model is used, which is intended to produce realistic wake profiles in yaw misalignment conditions [15].

Table 1: Mean turbine powers and offset for RAFT-FLORIS and FAST.Farm verification

	Mean Power (MW)		**Mean Surge (m)**		**Mean Sway (m)**	
	RAFT	**FAST.Farm**	**RAFT**	**FAST.Farm**	**RAFT**	**FAST.Farm**
T1	11.9	11.2	46.6	49.4	17.5	16.4
T2	6.6	5.6	36.3	35.1	0.6	-0.4
T3	12.6	11.9	62.4	64.6	0.6	0.3
T4	5.6	5.0	37.5	37.9	0.4	0.4

The mean power, surge, and sway for the four turbines are shown in Table 1 for the RAFT-FLORIS and FAST.Farm models. The RAFT-FLORIS coupling overpredicts the power for all four turbines, compared to FAST.Farm. This is likely because the wake models in FLORIS and FAST.Farm are not tuned to each other. However, the relative differences in power between turbines are well captured by the RAFT-FLORIS model. Turbine 3 shows the highest power because it is upwind and aligned with the wind while turbine 1 has a slightly lower power due to the yaw misalignment. Turbine 4 shows the lowest power, because it is directly downwind of turbine 3, and turbine 2 has an increased power because the wake of turbine 1 is directed away with yaw misalignment. The platform offsets in surge and sway are similar between the models, with a maximum difference of 6% for turbine 1 surge. Notably, the sway of turbine 1 under misaligned conditions is very similar between the models, which is most important for capturing the impacts of the floating offsets on the lateral wake deflection. These results verify the performance of the RAFT-FLORIS coupling for estimation of wind turbine power and offsets in yaw-misaligned conditions. The GCH wake model is applied in FLORIS for the rest of this paper. The choice of wake model impacts the magnitude of wake losses in downwind turbines, however it is not expected to influence the trend of results or the general findings on the impact of floating platform offsets on wake steering.

4 Results

To characterize the relationship between floating platform offsets and wake steering, we apply the RAFT-FLORIS coupling to a simple two-turbine case study. Again, the IEA 15 MW wind turbine and the VolturnUS-S semisubmersible are used. Within this two-turbine setup, the parameters are varied to quantify the impacts on power generation and wake steering effectiveness.

Platform offsets for floating wind turbines can vary significantly, depending on the chosen mooring system. To capture this variation, we developed a set of mooring systems with varying stiffness. The mooring systems are three-line taut-synthetic, designed for an 800 m depth and 1000 m anchoring radius. Taut synthetic mooring systems were chosen because of their linear response curve, which simplifies the behavior. The line stiffness was varied to achieve 12 mooring systems, ranging from very stiff to very compliant. The mooring system watch circles are shown in Figure 3, which maps the platform offset at maximum turbine thrust force in every direction. The mooring line stiffness was chosen such that the watch circle radius increases in approximately 25 m increments. In general, typical floating wind watch circles have a radius of less than 80 m. However in this work, the largest watch circles have radii greater than 200 m. It is likely that these platform offsets would need to be constrained due to the loads on the power cable; however, we chose to consider these very limiting cases to explore the full range of possible behavior. Additionally, the larger watch circles could be applicable for ultra-deep water scenarios, where larger platform offsets may be acceptable. Similarly, the very stiff mooring systems can be representative of more typical shallow-water systems or tension-leg platforms. The mooring systems are oriented such that one turbine is directly upwind of the second turbine. The turbines are spaced 1800 m apart (7.5 rotor diameters) and both have a mooring line directly upwind. In all cases, a 10 m/s wind is applied with a turbulence intensity of 0.06 with a heading toward positive X. The farm layout and wind flow field are shown in Figure 4 for three of the mooring systems, with a 25° yaw misalignment in the upwind turbine. The plot clearly shows how the wake of turbine 1 is

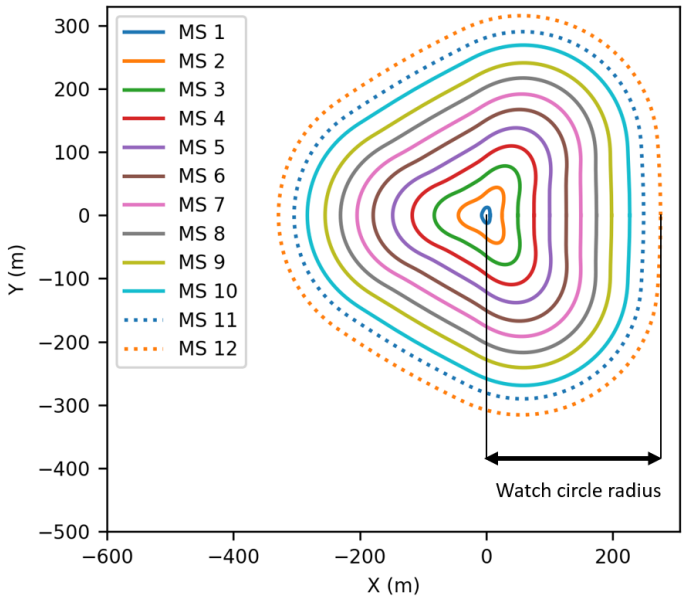

Figure 3: Mooring system watch circles

shifted, depending on the stiffness of the mooring system. Mooring system 1, the stiffest, shows minimal platform sway and results in behavior that is more reflective of fixed-bottom turbines. For mooring system 5, turbine 1 sways in positive Y, resulting in a shift in the center of the wake plane. This causes turbine 2 to experience much more of the wake than in the stiffer case. Mooring system 12, which has the most slack, allows significant sway motion in turbine 1 that exceeds the shift in wake center, and the wake effects on turbine 2 are decreased.

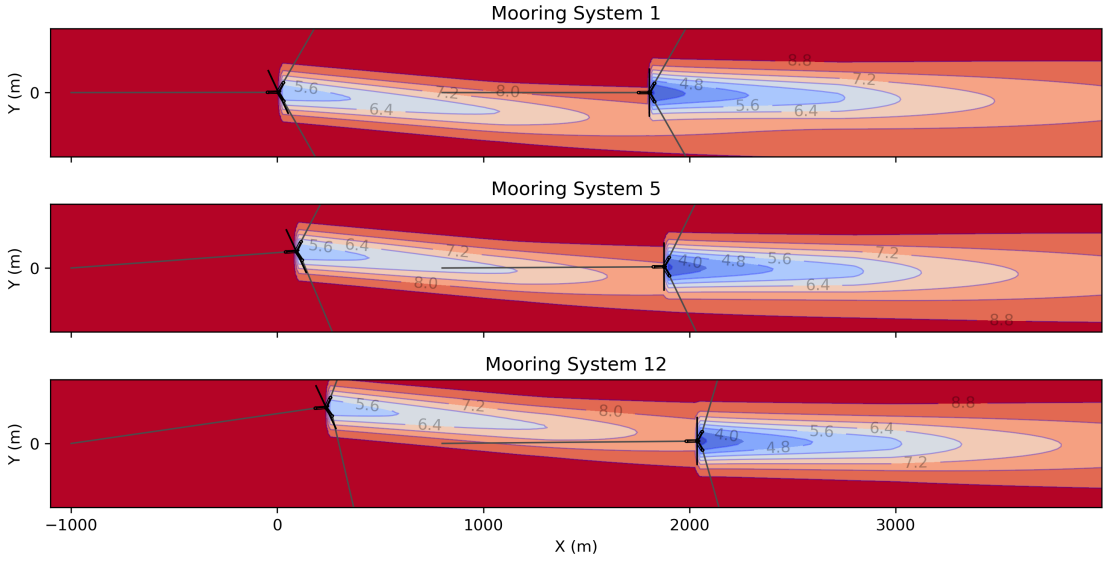

Figure 4: Wind flow field for mooring systems 1, 5, and 12 in 10 m/s wind with a 25° yaw misalignment angle in turbine 1

4.1 Turbine Power and Offsets

To further explore this, we apply the model to calculate the equilibrium positions of the mooring systems, with a range of yaw misalignment angles applied to turbine 1. The power for each turbine is mapped out in Figure 5. For turbine 1, the smaller yaw misalignment angles result in more power and stays consistent across increasing watch circles. The increase in platform pitch is minimal and does not have a noticeable impact on the power. The power for turbine 2 increases for increasing yaw misalignment angle because the turbine 1 flow is directed away. For a given yaw misalignment angle, the turbine 2 power decreases until reaching a minimum where the platform sway matches the shift in wake. Beyond this point, the turbine 2 power then increases with increasing watch circle because the turbine offset has overcome the wake shift. This reflects the wakes shown in Figure 4, where the offsets of turbine 1 are gradually shifting the wake center. For each yaw misalignment angle, there is a watch circle radius at which the power of turbine 2 is at a minimum. This non-optimal watch circle radius shifts larger as the yaw misalignment angle increases because larger yaw misalignment angles lead to a larger wake deflection and require larger platform sway offsets to overcome.

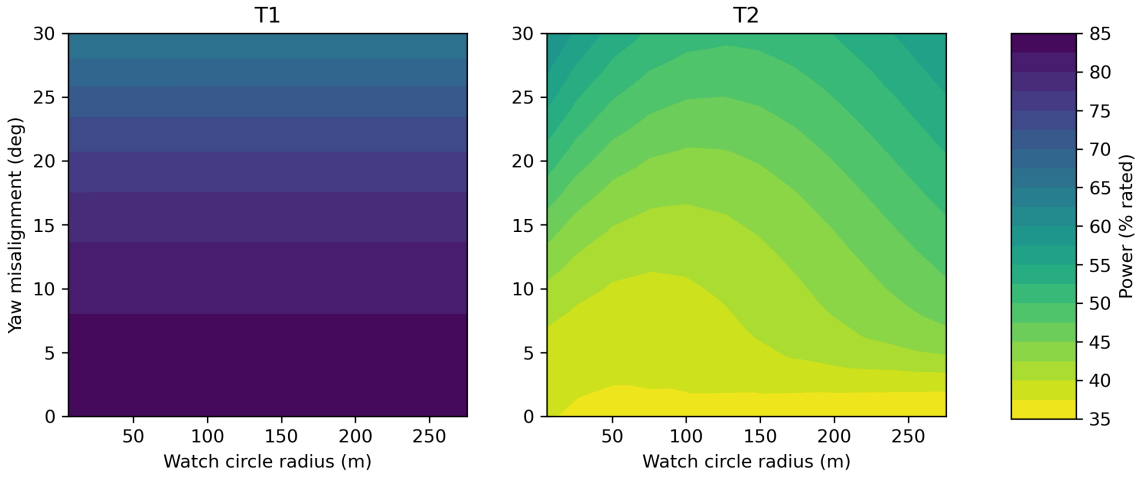

Figure 5: Heatmaps of turbine power for varied watch circle radius and yaw misalignment angle

The turbine 1 sway is mapped for the same range of watch circle and yaw misalignment angles in Figure 6. For larger watch circles, the sway offsets increase, ranging from nearly 0 m for the most stiff mooring system to 180 m for the most slack mooring system. At smaller yaw misalignment angles, the turbine sway shows significant variation before leveling out at larger yaw misalignment angles. Figure 6 also shows the total farm power, which sums the power of turbine 1 and 2. The smallest watch circle (6 m radius) approximates a fixed-bottom case. In this case, the yaw misalignment is beneficial for total farm power until reaching a peak at about 22°. As the watch circles increase in size, the total farm power decreases and then increases, similar to the behavior seen in turbine 2 power. The minimum farm power occurs for the largest yaw misalignment angle of 30 ° and a watch circle radius of around 100 m, where both turbine 1 and 2 are disadvantaged, with a large loss of power in turbine 1 due to the yaw misalignment and a loss of power in turbine 2 because the lateral wake deflection and sway offsets are cancelling out. There is a gain in total farm power for very large watch circles, when the sway offsets have far exceeded the lateral wake deflection.

At a 0° yaw misalignment angle, there is a small decrease in total farm power for larger watch circles. This is because for larger watch circles, the relative spacing between turbine 1 and turbine 2 decreases by up to 100 m compared to the smallest watch circle. The impact of platform pitch is minimal, as the pitch changes by less than 1° across the systems. For more typical watch circles of less than 100 m radius, there is minimal change in total farm power at 0° yaw misalignment. This confirms that floating platform offsets can generally be disregarded when they are offsetting in the direction of the wind.

4.2 Mooring System Orientation

The relationship between the platform offset at different yaw misalignment angles is highly dependent on the mooring system orientation relative to the wind direction. Figure 7 shows the turbine offset

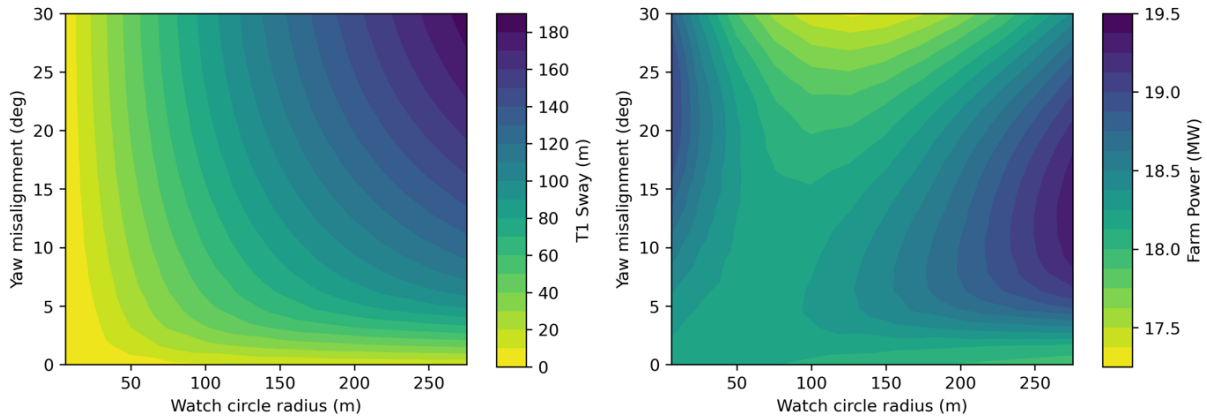

Figure 6: Heatmap of turbine 1 sway and total farm power for varied watch circle radius and yaw misalignment angle

position for yaw misalignment angles ranging from 0° to 30° for three orientations of mooring system 9. Mooring system 9 is one of the most slack designs, so the offsets are exaggerated relative to more typical mooring designs. The figure shows that the turbine offset position under misaligned conditions varies significantly depending on the mooring system rotation. For a 0° mooring system orientation, the platform offsets significantly in positive Y. The change is most significant for smaller yaw misalignment angles. This occurs because the restoring force in Y is minimal in the primary loaded line (the upwind mooring line). The 0° mooring system reflects the results show in the previous heatmaps.

For a 30° mooring system rotation, the platform sway motions are smaller than in the 0° case. For small yaw angles, the platform offsets in negative Y, even though the aerodynamic force has a positive Y component. This is because the primary loaded line has a larger negative Y component than the aerodynamic force. Only the 30° yaw angle causes significant sway motions for this mooring system orientation.

For a 60° mooring system rotation, the turbine offsets are approximately perpendicular to the rotor plane for all yaw misalignment angles. The sway motions for this mooring system orientation are much smaller than those of the 0° rotation. In this case, the restoring force is split over two mooring lines that balance out each other's Y contributions. These results highlight the importance of considering mooring system orientation when evaluating wake steering and platform offsets in floating wind turbines.

To understand the sensitivity of the mooring system orientation on the wake losses, we rotate both mooring systems 0°, 30°, and 60°and evaluate the impact on turbine 2 power. The spacing remains the same at 1800 m and turbine 1 is still directly upwind of turbine 2. Figure 8 plots the turbine 2 power for the three mooring system orientations and for three turbine 1 yaw misalignment angles. The 0° rotation reflects the results shown in Figure 5, with the turbine 2 power first decreasing then increasing as the watch circle increases. This reflects the shift of the wake center as turbine 1 sways significantly under the yaw-misaligned loading.

For the 30° and 60° rotations, the results differ significantly. For a 10° and 20° yaw misalignment angle, the increasing watch circle radius decreases the turbine 2 power for all watch circle sizes. This is because the turbine 1 sway offsets are minimal for these orientations and shift the wake center closer to turbine 2. For a 30° yaw misalignment, the 30° mooring system rotation does show a similar response to the 0° mooring system. This is because turbine 1 sways significantly in these conditions, as shown in Figure 7, and eventually deflects the wake beyond turbine 1.

4.3 Turbine Spacing

Finally, we evaluate the impact of turbine spacing in Figure 9, where the turbine 2 power is plotted against watch circle radius for turbine spacings ranging from 1200 to 2400 m, and three turbine 1 yaw misalignment angles. Here, the 0° mooring system orientation is again used, with a mooring line directly upwind. The 1800 m case is the spacing used in the previously provided results. The turbine 2 power increases with increasing turbine spacing for all mooring systems. The impact of watch circle radius on turbine 2 power is much more pronounced for smaller turbine spacings. The larger turbine

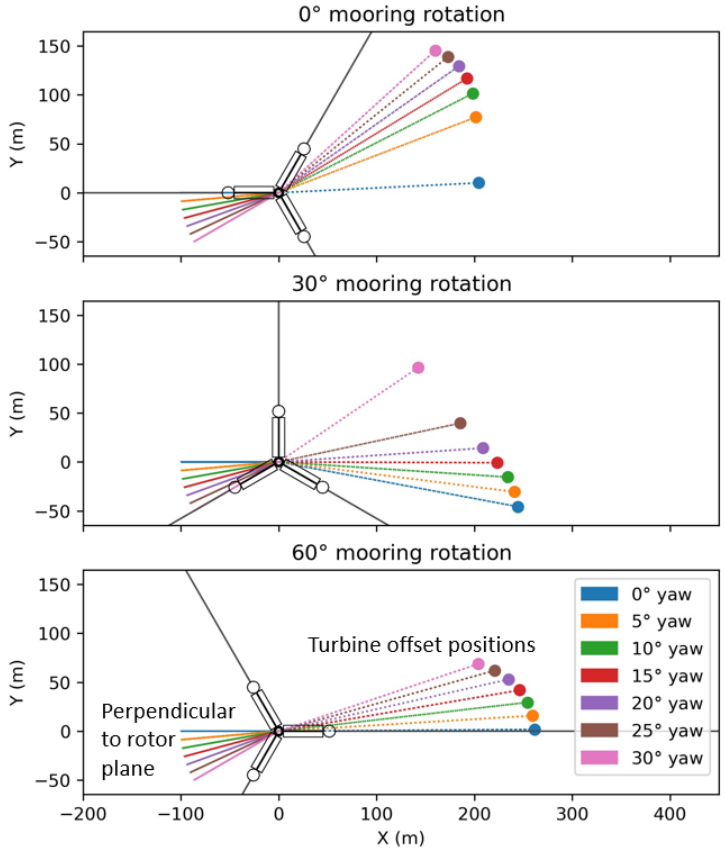

Figure 7: Turbine offset positions for mooring system 9 at 0°, 30°, and 60° mooring system rotations

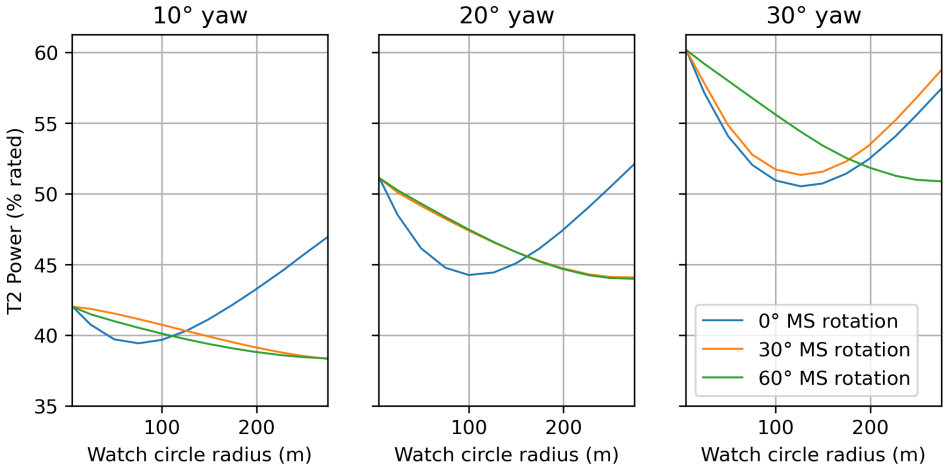

Figure 8: Turbine 2 power for mooring system rotations of 0°, 30°, and 60°, and three yaw misalignment angles of 10°, 20°, and 30°

spacings allow more room for the wake to dissipate, so the impact is lessened. For the 20° and 30° yaw misalignment cases, the mooring systems with extreme offsets eventually overcome the power losses from the reduced turbine spacing.

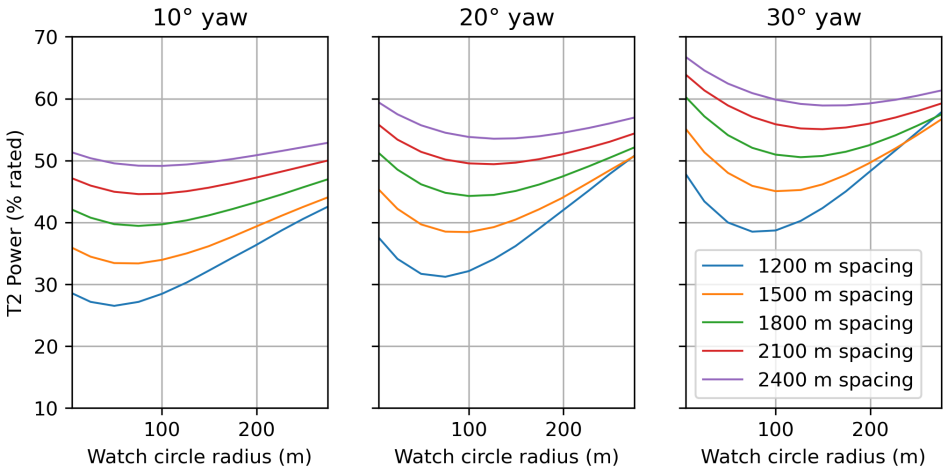

Figure 9: Turbine 2 power for varied turbine spacings of 1200 m to 2400 m, and three yaw misalignment angles of 10°, 20°, and 30°

5 Conclusions

This paper presents a novel tool for the coupled modeling of floating platform offsets and wake effects, especially considering the impacts on wake steering. The tool couples RAFT, a frequency-domain wind turbine model, and FLORIS, a steady-state wake modeling tool. A verification of the tool with FAST.Farm confirms accurate platform offsets and relative turbine powers in yaw misalignment scenarios. The tool is then applied to a simple two-turbine scenario with one turbine directly upwind, where the yaw misalignment angle is varied. We consider a set of mooring systems, with stiffness ranging from very stiff to very slack, which is reflected in increasing watch circle radius. This allows us to map out patterns in turbine power across a range of watch circle sizes and yaw misalignment angles. For a mooring system oriented with a line directly upwind, the results show that the platform offset under yaw-misaligned conditions can counteract the benefits of wake steering. For a given yaw misalignment angle, there is a watch circle radius that results in a minimum power in the downwind turbine, where the platform sway and wake shift match. This non-optimal watch circle radius varies for different yaw misalignment angles and turbine spacings. Additionally, the results highlight the sensitivity of the mooring system orientation relative to wind direction in wake steering performance. The offset position of the platform under yaw-misaligned forces differs significantly, depending on the mooring system orientation relative to the wind direction. For a mooring system with a line directly upwind, the sway offsets are large, even for small yaw misalignment angles. For a mooring line oriented with a line directly downwind, the sway offsets are much smaller, even with large yaw misalignment angles. This change in offsets then impacts the wake steering effectiveness, where a mooring system with a line directly downwind experiences reduced downwind power generation for increasing watch circles. These results show the importance of considering floating platform offsets when evaluating wind farm control strategies. In future work, floating offsets and the mooring system should be included in layout and wake steering optimizations. Additionally, this analysis should be repeated with catenary and asymmetrical mooring systems, which have more nonlinear response curves and can differently impact platform offsets.

Acknowledgments

This work was authored in part by the National Renewable Energy Laboratory, operated by the Alliance for Sustainable Energy, LLC, for the U.S. Department of Energy (DOE) under Contract No. DE-AC36-08GO28308. Funding provided by the U.S. Department of Energy Office of Energy Efficiency and Renewable Energy Wind Energy Technologies Office. The views expressed in the article do not necessarily represent the views of the DOE or the U.S. Government. The U.S. Government retains and the publisher, by accepting the article for publication, acknowledges that the U.S. Government retains a nonexclusive, paid-up, irrevocable, worldwide license to publish or reproduce the published form of this work, or allow others to do so, for U.S. Government purposes.

References

[1] Fleming P, Annoni J, Shah J J, Wang L, Ananthan S, Zhang Z, Hutchings K, Wang P, Chen W and Chen L 2017 *Wind Energy Science* **2** 229–239

[2] Fleming P A, Ning A, Gebraad P M and Dykes K 2016 *Wind Energy* **19** 329–344

[3] Wise A S and Bachynski E E 2020 *Wind Energy* **23** 1266–1285

[4] van Binsbergen D W, Wang S and Nejad A R 2020 Effects of induction and wake steering control on power and drivetrain responses for 10 mw floating wind turbines in a wind farm *Journal of Physics: Conference Series* vol 1618 (IOP Publishing) p 022044

[5] Johlas H, Martínez-Tossas L A, Lackner M, Schmidt D and Churchfield M J 2020 Large eddy simulations of offshore wind turbine wakes for two floating platform types *Journal of Physics: Conference Series* vol 1452 (IOP Publishing) p 012034

[6] Kheirabadi A C and Nagamune R 2019 Modeling and power optimization of floating offshore wind farms with yaw and induction-based turbine repositioning *2019 American Control Conference (ACC)* (IEEE) pp 5458–5463

[7] Kheirabadi A C and Nagamune R 2020 *Ocean Engineering* **208** 107445

[8] Hall M, Housner S, Zalkind D, Bortolotti P, Ogden D and Barter G 2022 An open-source frequency-domain model for floating wind turbine design optimization *Journal of physics: conference series* vol 2265 (IOP Publishing) p 042020

[9] Gebraad P, Fleming P, Ning S A and van Wingerden J W 2014 Floris, version 00 URL `https://www.osti.gov//servlets/purl/1262644`

[10] Ning S A 2013 URL `https://www.osti.gov/biblio/1260115`

[11] Jonkman J M and Shaler K 2021 *Fast. farm user's guide and theory manual* (National Renewable Energy Laboratory Golden, CO, USA)

[12] Gaertner E, Rinker J, Sethuraman L, Zahle F, Anderson B, Barter G E, Abbas N J, Meng F, Bortolotti P, Skrzypinski W *et al.* 2020 Definition of the IEA 15-Megawatt offshore reference wind turbine Tech. rep.

[13] Allen C, Viscelli A, Dagher H, Goupee A, Gaertner E, Abbas N, Hall M and Barter G 2020 Definition of the umaine volturnus-s reference platform developed for the iea wind 15-megawatt offshore reference wind turbine Tech. rep.

[14] Fleming P, King J, Bay C J, Simley E, Mudafort R, Hamilton N, Farrell A and Martinez-Tossas L 2020 *Journal of Physics: Conference Series* **1618** 022028 ISSN 1742-6588, 1742-6596 URL `https://iopscience.iop.org/article/10.1088/1742-6596/1618/2/022028`

[15] Branlard E, Martínez-Tossas L A and Jonkman J 2023 *Wind Energy* **26** 44–63